Astrosat-CZTI

Santosh Vadawale
Physical Research Laboratory
Ahmedabad

On behalf of CZTI Team

Advanced AstroSat Data Analysis Workshop, 29 June 2021

Outline

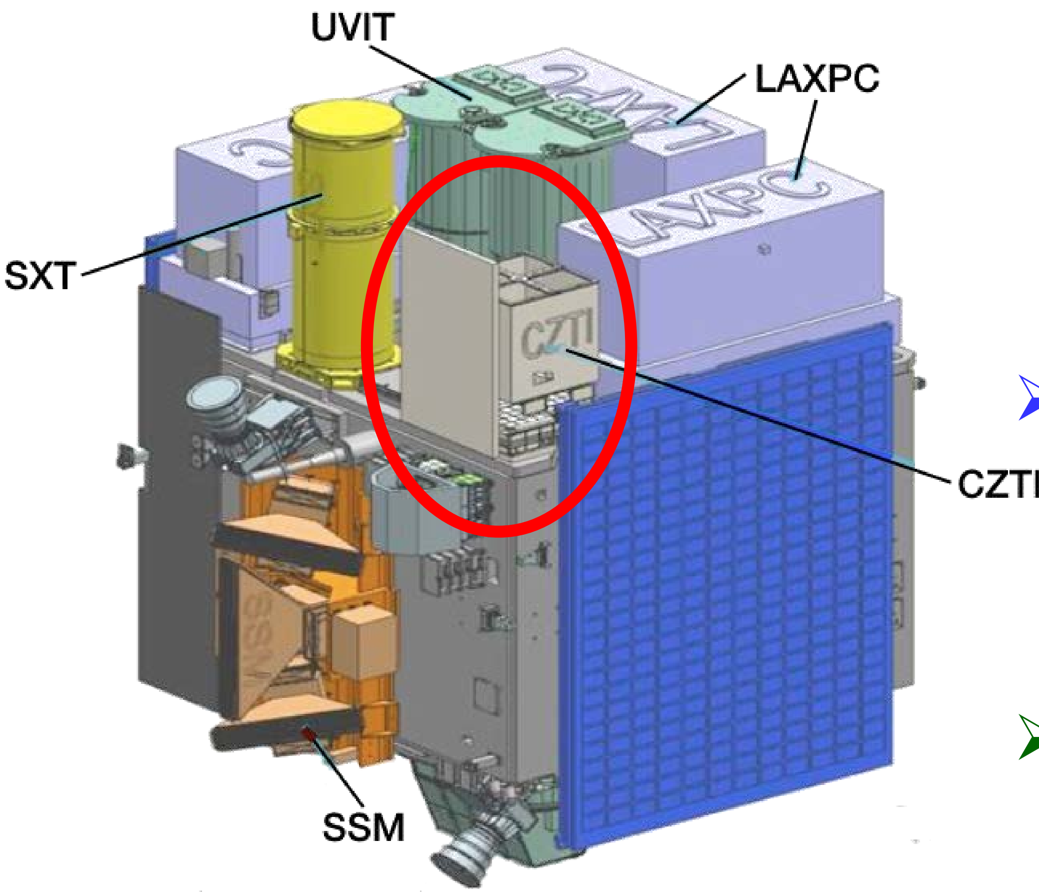

- Astrosat CZTI
  - Brief introduction
  - Imaging technique
  - CZT detectors
  - Calibration
  - In-flight 'Observations'
- X-ray polarimetry
  - Brief Introduction
  - Hard X-ray polarimetry with CZTI
- CZTI as GRB detector
  - GRB polarimetry
  - EMGW monitoring → DKASHA
- Summary

Astrosat CZTI

Hard X-ray Spectroscopy and Imaging

Coded Mask imaging with pixilated CZT detectors

- Detector plane area: 976 cm^2
- Pixel size: 2.46 x 2.46 mm^2
- Total number of pixels: 16384
- Detector thickness : 5 mm

➤ Mask and support structure designed for shielding up to ~100 keV

➤ Detectors have significant efficiency upto ~400 keV

➤ Results in additional capabilities

→ Hard X-ray transient monitoring

→ **Hard X-ray polarimetry**

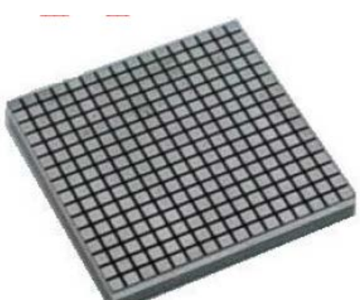

CZTI Configuration

Four Independent Quadrants

- Total 64 modules (16 in each quadrants)
- ASIC based readout (2 x 128 ch. ASIC)
- Two FOVs:
  $4.67° \times 4.67°$
  $\sim 80° \times 80°$

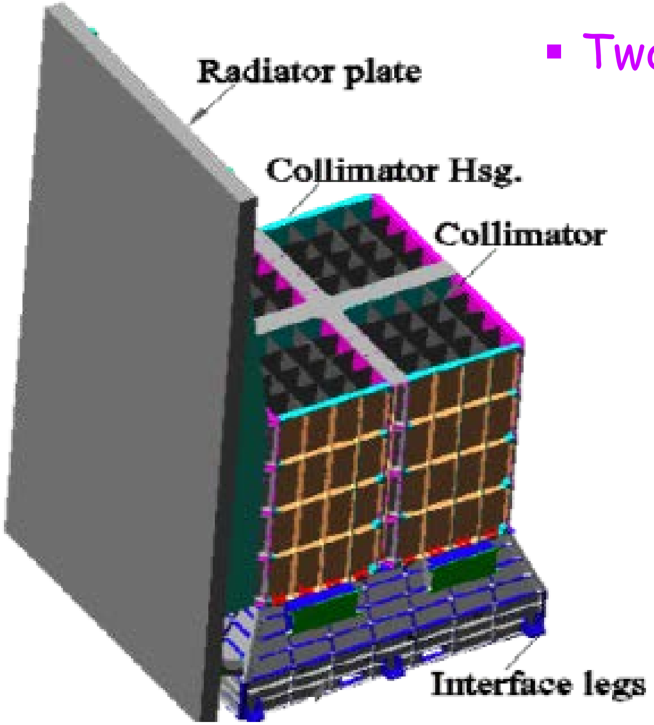

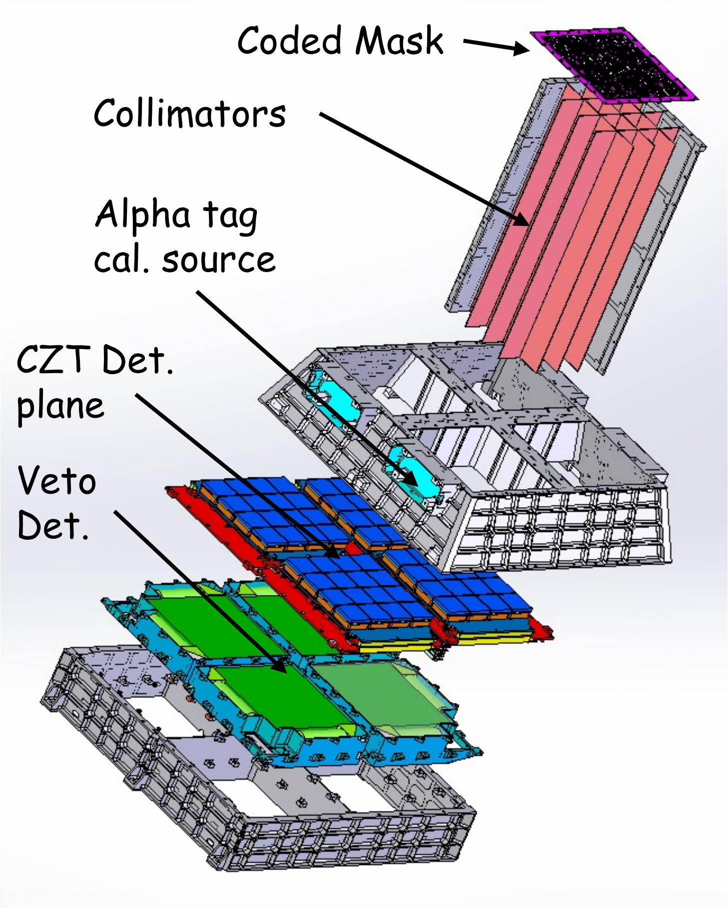

- Size: 484 x 484 x 600 mm^3
- Weight: 50 kg Power: 50 Watts

Hard X-ray Astronomy

- No flux concentration ➔ *Always background dominated*
  - *Accurate background knowledge is essential*
- Mostly continuum spectroscopy
  - *Accurate knowledge of detector response is essential*

CZTI Salient Features

- Indirect imaging with coded aperture mask
  - 8′ angular resolution, simultaneous background measurement
- Mask and shielding designed up to 100 keV
  - Hard X-ray monitoring above ~100 keV
- Time tagged event data with 20 μs accuracy
  - Allows Compton spectroscopy and polarimetry
- Alpha-tagged detector for onboard calibration
- Veto detector for additional background rejection
- Low inclination orbit
- Absolute time correlation with onboard SPS

Coded Mask Imaging

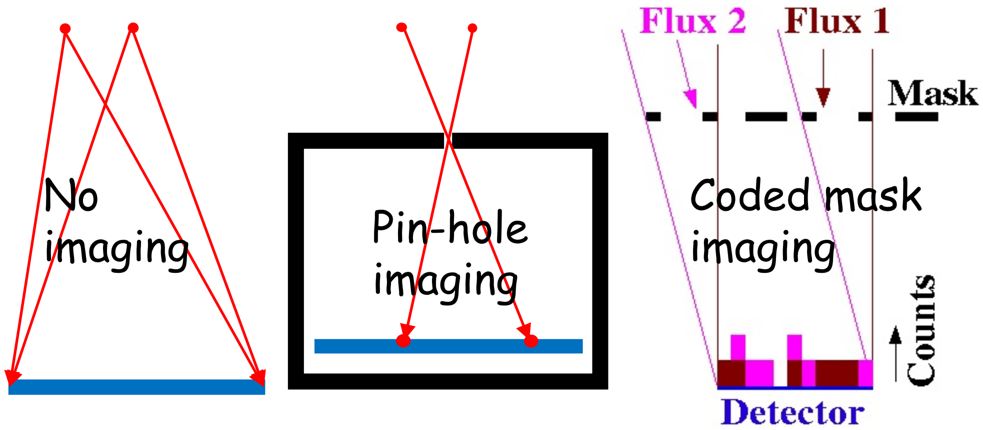

- In-direct imaging technique
- Uses mask shadow pattern
- Angular resolution determined by mask pixel size and mask to detector distance

Mask (M)

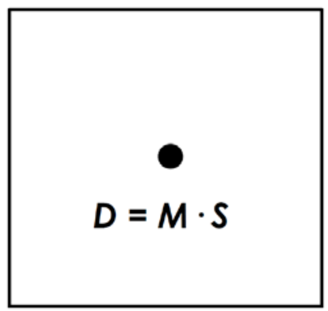

Sky (S)

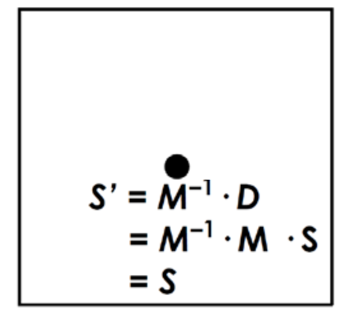

In real world

- Mask pattern is not invertible matrix
- Detector has significant background
- Detector plane is not uniform / ideal

➔ Reconstructed images are not perfect

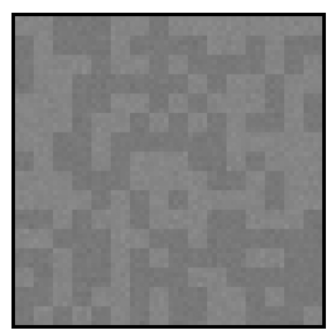

Detector Response (D)

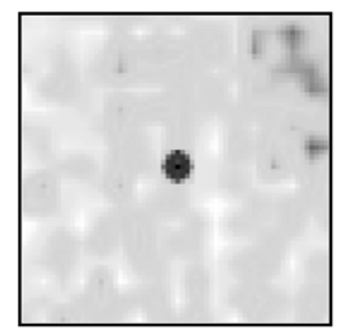

Reconstructed Sky Image (S')

Coded Mask Patterns

- ➢ Random pattern → simplest mask, ~50 % open fraction, slideloabs
- ➢ Uniformly Redundant Array (URA) → flat slidelobes, ghosts

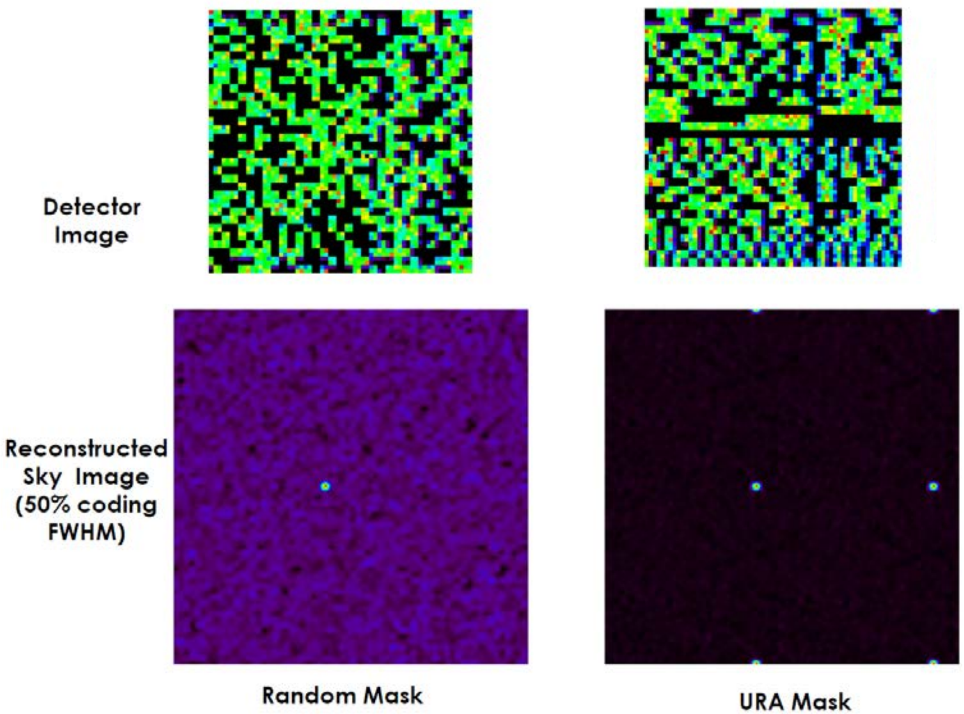

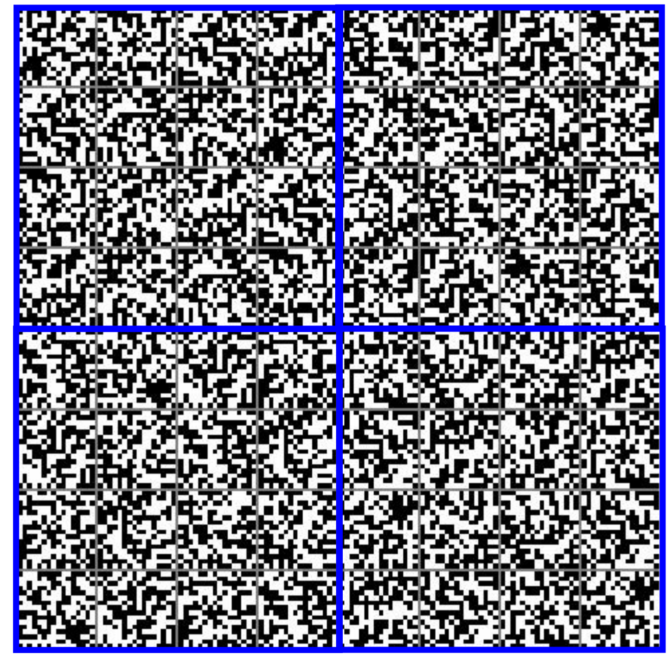

CZTI Coded Mask

- ➢ CZTI employs 16 x 16 URA variant → One for each detector module
- ➢ 7 different URA patterns are to make mask pattern for one quadrant.
- ➢ The same pattern is used for other quadrants with 90 deg. Rotation.
- ➢ Different methods of image reconstruction → FFT, cross correlation, back projection, Bayesian → CZTI Pipeline uses FFT

CZT Detector Modules

Best candidate for large area position sensitive detector required for coded aperture imaging

Semi-conductor detector

- Lower energy per e^-/h^+ pair
  - Better energy resolution
- High band gap energy then Si/Ge
  - Near room temp. operation
- High efficiency
  - higher energy range
- No intrinsic amplification
- Different e^-/h^+ mobility
  - Asymmetric line shape

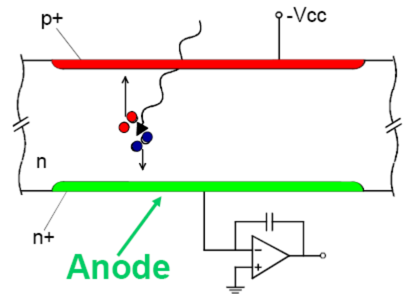

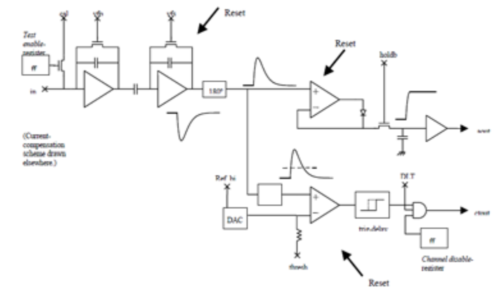

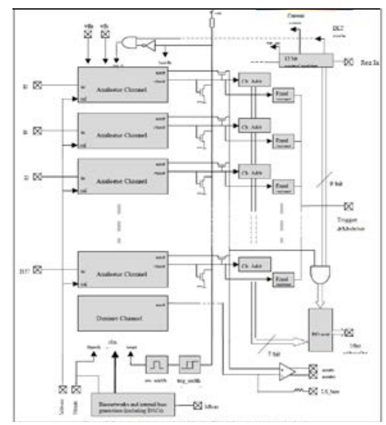

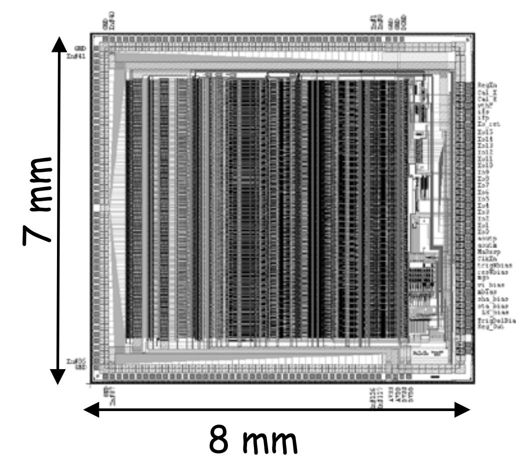

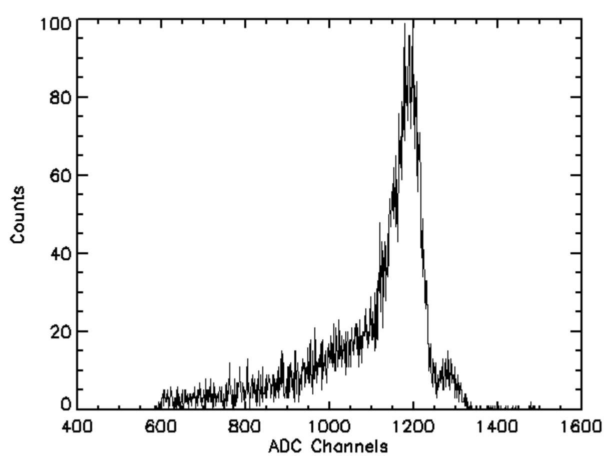

- Smaller pixel size
  - Better imaging and spectroscopic performance
- Large number of pixels
  - ASIC based readout essential
  - Each pixel is independent detector

CZT line shape

Hecht Equation

For non-pixilated detector

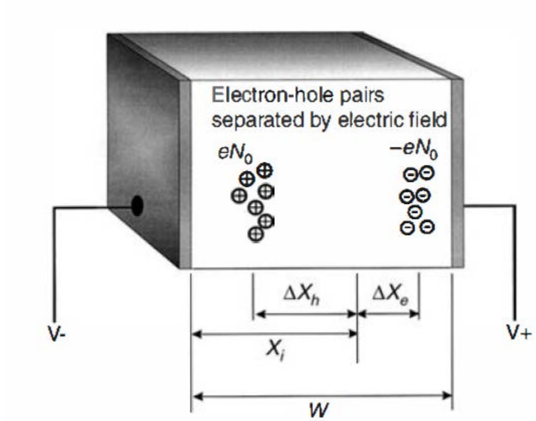

$$Q^* = eN_0\left\{\frac{v_h\tau_h^*}{W}\left(1-\exp\left[\frac{-x_i}{v_h\tau_h^*}\right]\right)+\frac{v_e\tau_e^*}{W}\left(1-\exp\left[\frac{x_i-W}{v_e\tau_e^*}\right]\right)\right.$$

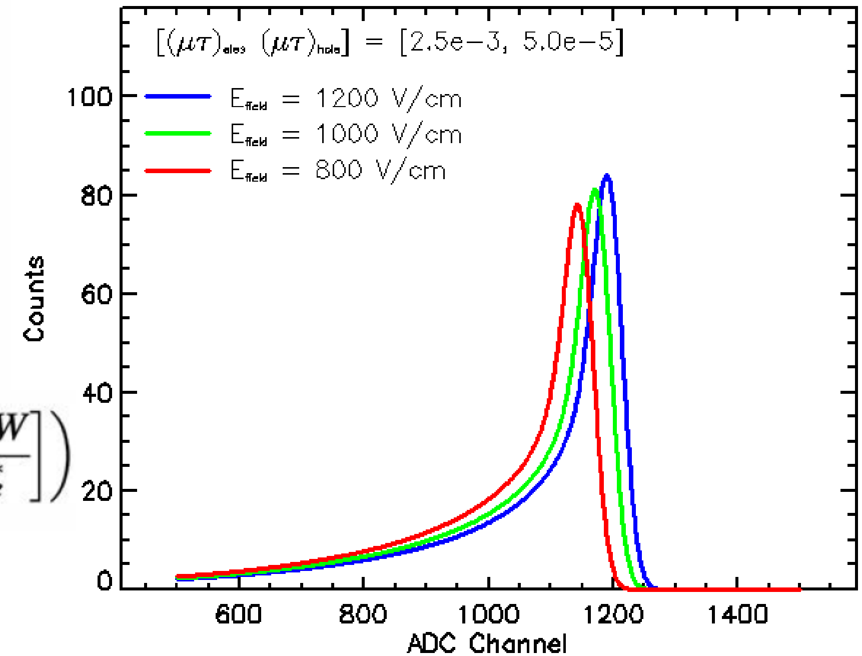

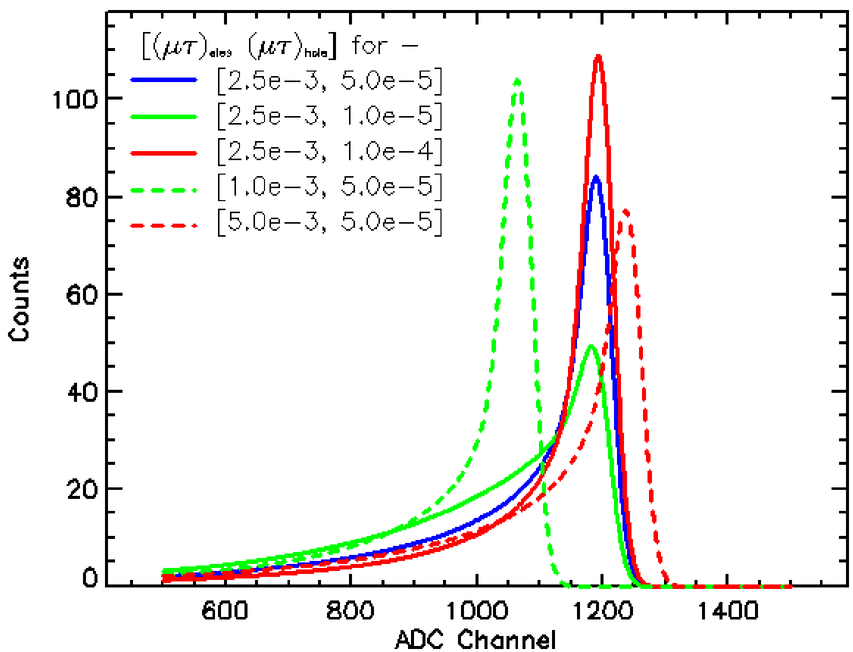

Six input parameters to be measured experimentally

- $\mu\tau_{\text{-electron}}$
- $\mu\tau_{\text{-hole}}$
- Electric field
- Energy resolution
- Electronics gain
- Offset

CZT Detector Response

- CZTI line profile is not Gaussian
- Standard Hecht equation based model
  - under predicts tail at low energies for multi-pixel crystals
- Essential to consider charge sharing across pixels

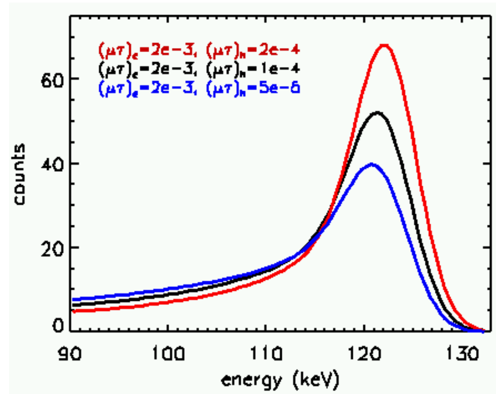

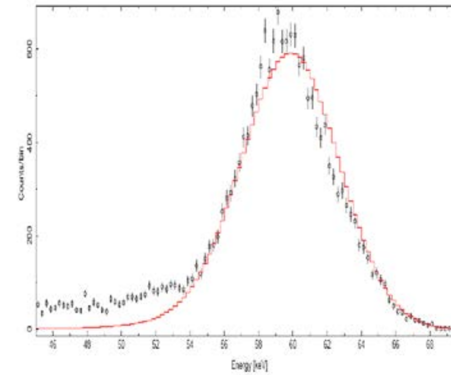

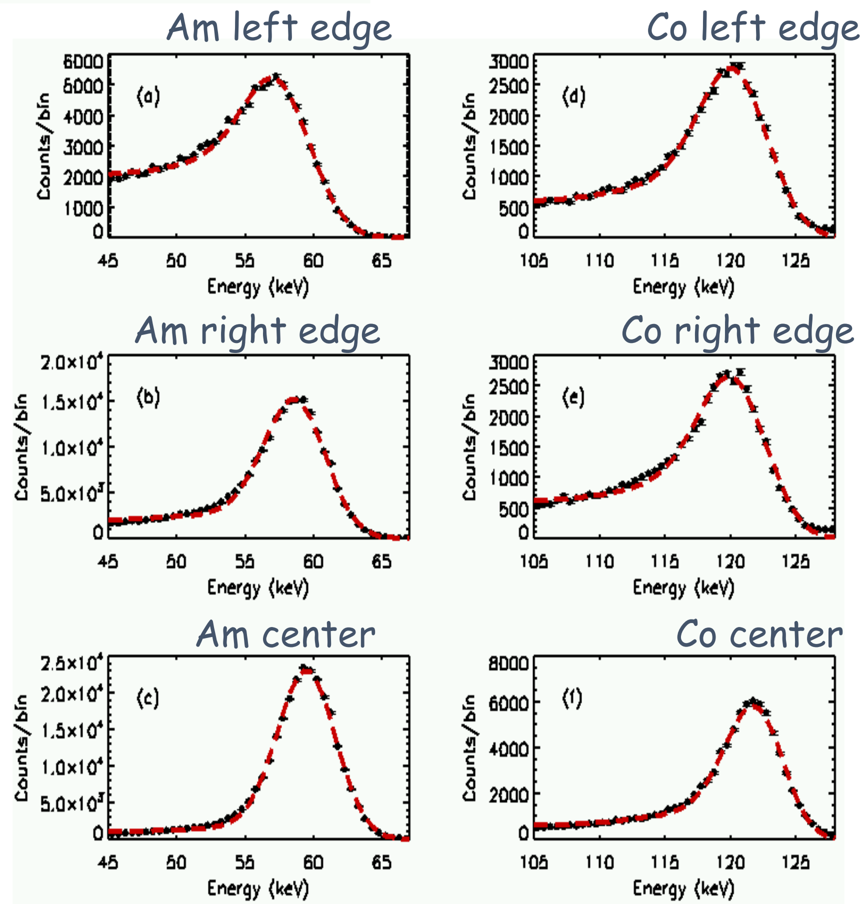

New CZTI Line model validation

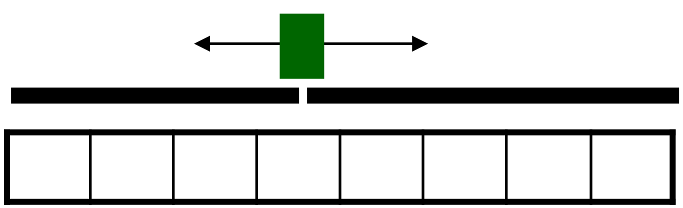

- Slide a 100 μm slit across pixels with accuracy of 50 μm
- Simultaneous fit of spectra at edges and center at two energies

CZTI Response Matrix

- ➢ Model implemented in ISIS
  - ▪ Simultaneous fit to spectra at three energies for all pixels at five temp.
- ➢ Total ~80000 spectral fits Using PRL Vikram-100 HPC cluster
- ➢ Proper Fitting ~90% of the pixels to obtain model parameters
  - ▪ Rest flagged spectroscopicallly bad

Key parameter for all pixels

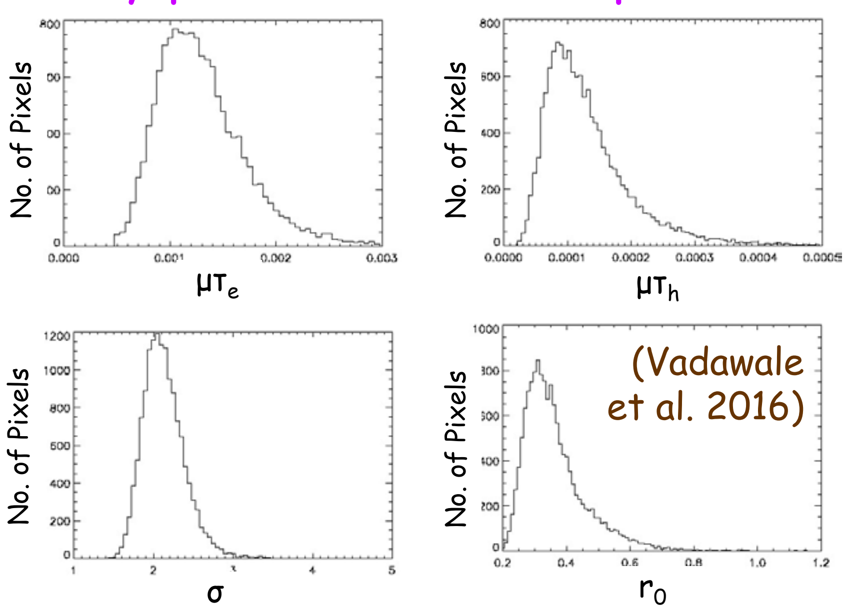

(Vadawale et al. 2016)

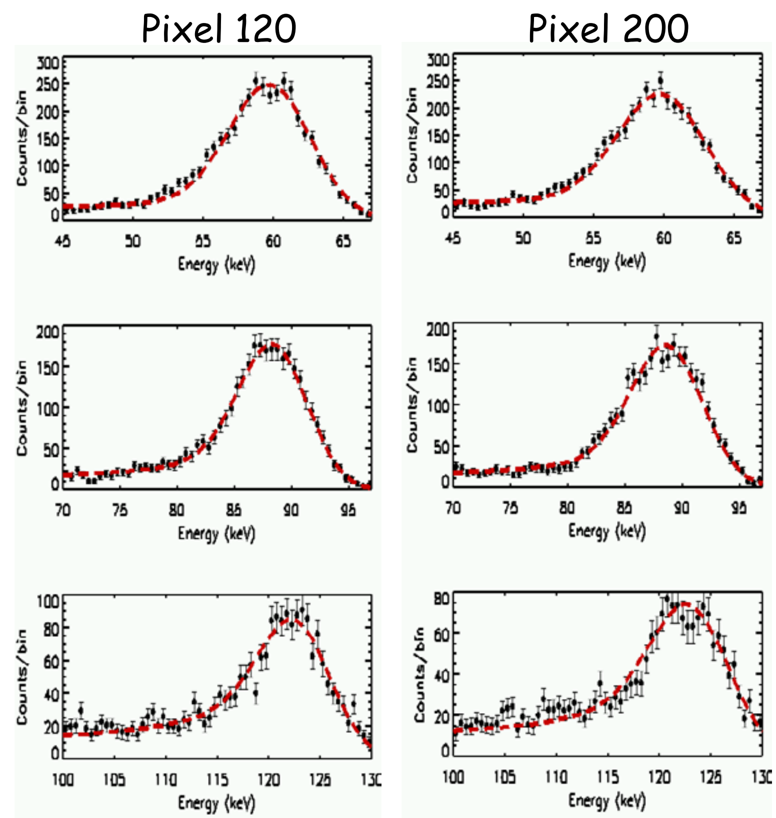

- ➢ Group similar pixels
  - ▪ Compute redistribution matrix for each group
- ➢ All parameters and matrices stored in CALDB
- ➢ Final multi-pixel response matrix ➔ Weighted addition

Spectroscopy with Coded Mask

Mask-weighting

- Data dominated by background events
- Simultaneous measurement of background from masked pixels
- Mask weighting technique for background subtracted source spectrum

Mask-weighted spectrum:
Background subtracted source spectrum per fully illuminated unit area on the detector plane (similar to Swift BAT)

$$f_i = \text{Mask open fraction of pixel } i$$
$$a_i = \text{Effective area including QE of pixel } i$$
$$B_i = \text{Relative background level of pixel } i$$
$$C_i = \text{Count in pixel } i$$

D ➔ Renormalization factor

N ➔ *Area rescaling for a given pointing*

Recalculated when pointing offset changes by a fixed value (3')

→To account for S/C jitter

Coming up

- Revised algorithm (next version)
- Include energy dependent background
- No more area rescaling

➔ Spectrum in terms of observed counts

CZTI In-flight observations

CZTI In-flight 'Observations'

'Bunch' Events

- First observations showed ~10 times higher count rate
- Variance is not Poissonian
- All events are not "independant", both temporally and spatially

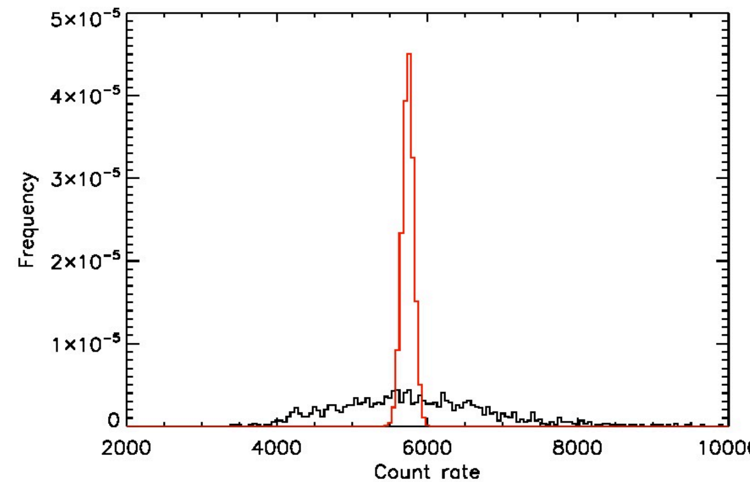

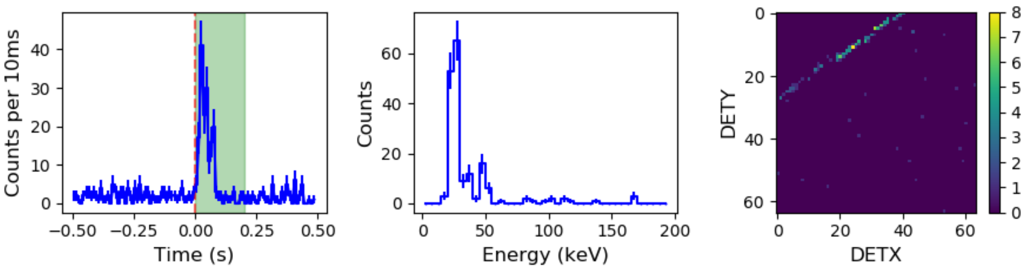

(Ratheesh et al. 2021)

- Similar effect in other missions → Integral (PICsIT)
- Possible to identify by clever algorithm

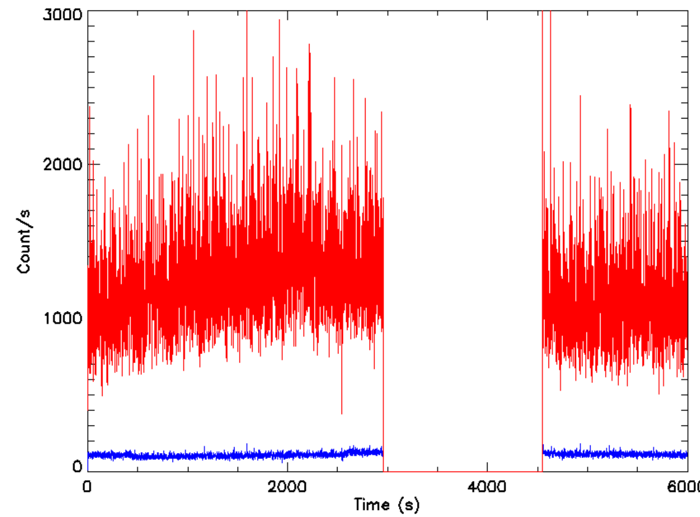

(Vadawale et al. 2016)

➔ Advantage of having time tagged event information unlike earlier experiments (RT-2/Chronos-Photon, HEX/Ch-1)!!

Onboard bunch cleaning from Feb 16 by a firmware patch

CZTI In-flight 'Observations'

Anomalous pixels

- A fraction of pixels have anomalously low count rates since first day
- Tantalum lines and 60 keV line are not seen in the same pixels
- Gain of those pixels changed drastically–threshold ~70 keV !!
- ~20% of pixels ➔ flagged as spectroscopically bad in CALDB

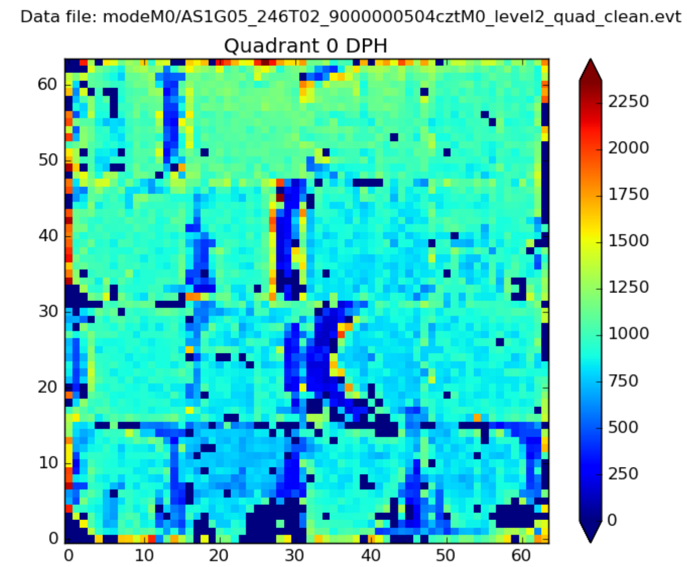

Background non-uniformity

- Background not expected to be uniform by design
- Knowledge of this non-uniformity important for effective background subtraction
- Multiple blank sky observations used to derive the fixed patterns of background in the detector plane

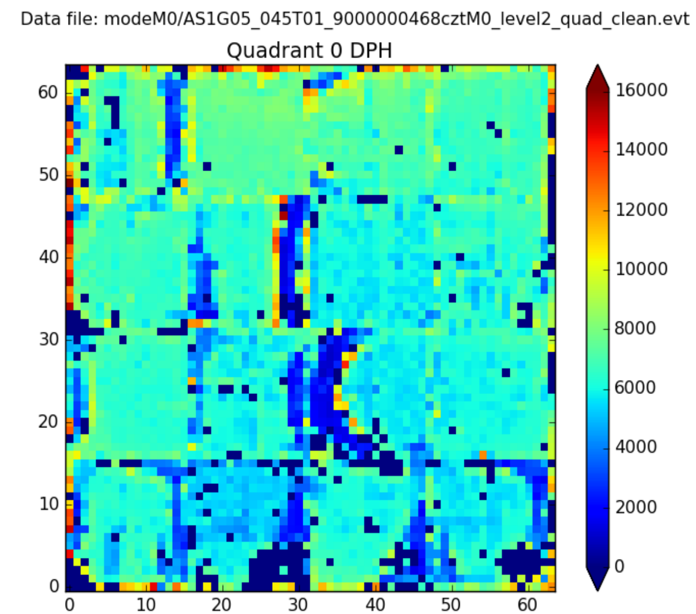

CZTI In-flight 'Observations'

Different images in all of quadrants

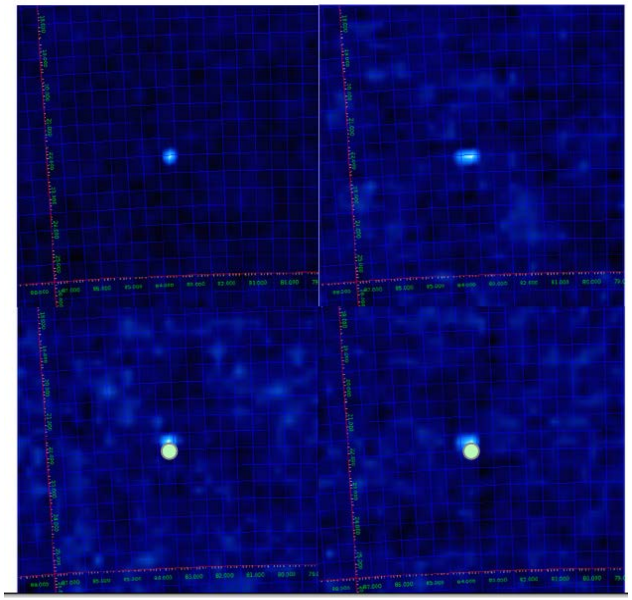

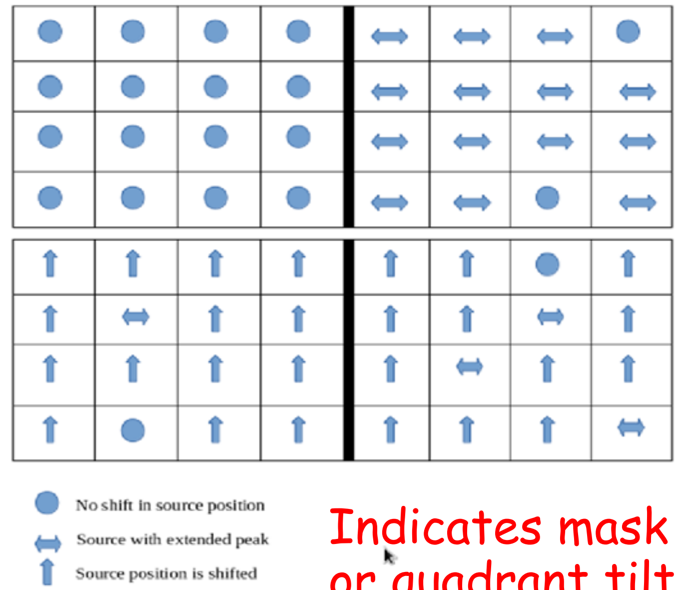

Indicates mask shifts or quadrant tilts

- Imaging by cross-correlation of different crab observations
- Module level imaging to identify the image shifts – measure boresight
- Consistent results across multiple observations
- Account for flux discrepancy

Quadrant	X Shift (mm)	Y Shift (mm)
Q0	0.00	0.00
Q1	-1.45	0.00
Q2	0.00	1.68
Q3	0.00	1.50

(Vibhute et al. 2021)

CZTI In-flight 'Observations'

In-flight gain calibration

- Alpha-tag source → Am-241 source encapsulated in CsI crystal
- Spectrum of 59.6 keV line using alpha tagged events
- Background spectrum has Ta K-alpha and K-beta peaks
- Three lines for in-flight calibration
- Pixel gain measurement

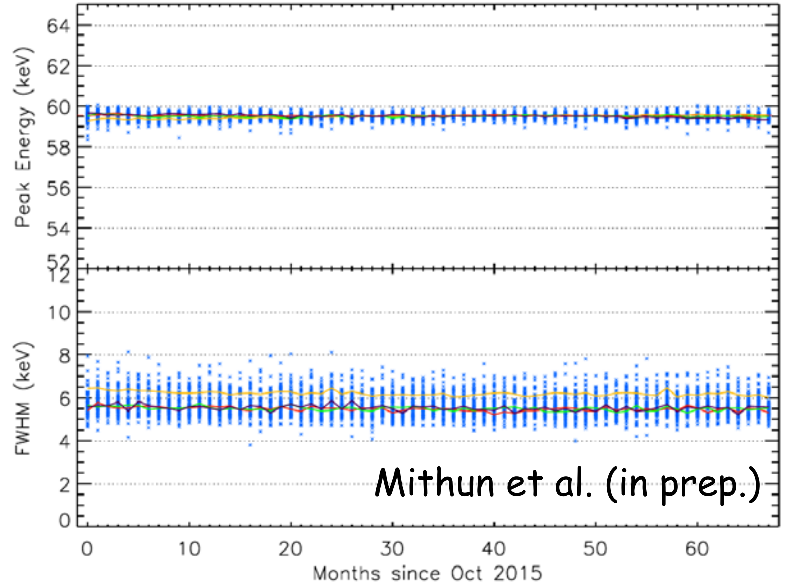

Low energy threshold (LLD)

- Each of the detector module has a configurable LLD
- Pixel to pixel gain vairiations will make actual LLDs in PI space for each pixel different
- Pixel wise LLD measurement required for response → automated measurements

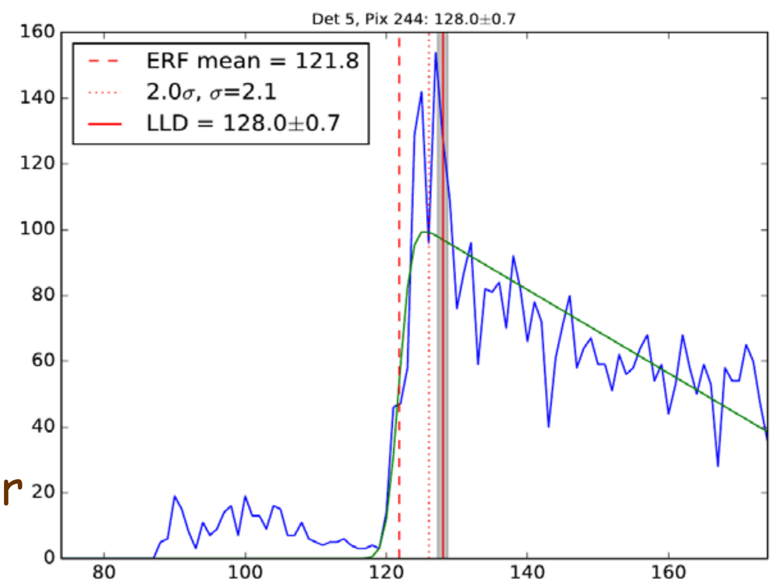

All parameters stored in CALDB → Standard HEASARC Caldb file structure

Crab spectrum: All Quadrants

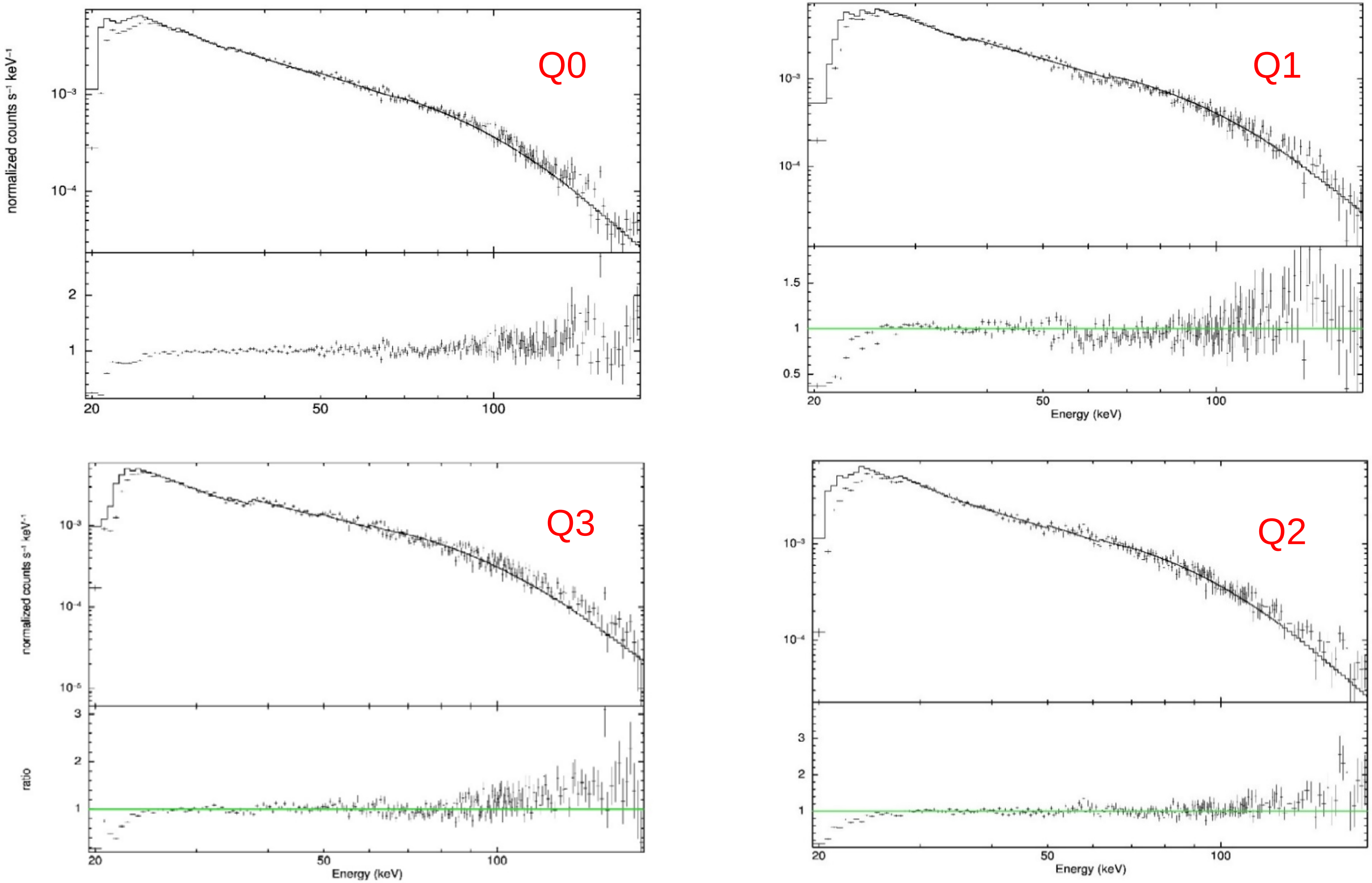

Cross calibration with NuSTAR

- PI: 2.09+- 0.0015; Norm (FPMA) – 7.97455+- 0.025
- CZTI Q0 norm – 0.87 * NuSTAR FPMA

Hard X-ray polarimetry with CZTI

Specific Details of CZTI data analysis by Shah Alam

X-ray Polarimetry

- X-ray observations so far use three main attributes
  - ➔ Energy, direction, arrival time
- Astrophysical X-rays have two more independent attributes
  - ➔ Polarization fraction, polarization direction

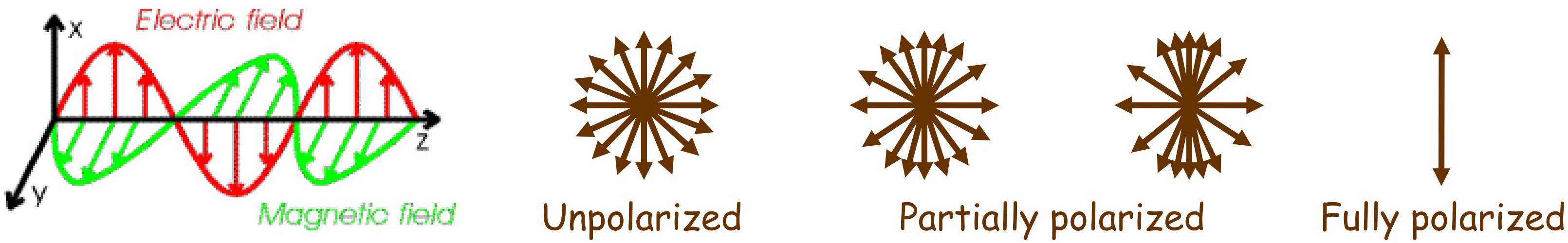

- Can provide vital information on radiation processes, geometry, magnetic fields
- Not used effectively so far

- Importance of polarimetric observations known from early days of X-ray astronomy
- First attempts by rocket flights in late 1960s
- Only dedicated satellite experiment in 1975 on-board OSO-8
- Few experiments attempted later by could not succeed due to various reasons
- Two dedicated missions in next couple of years

How to measure X-ray polarization

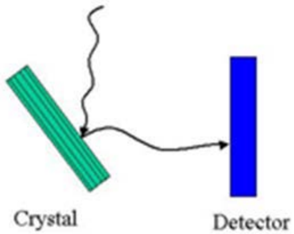

Brag reflection

Photo-electric

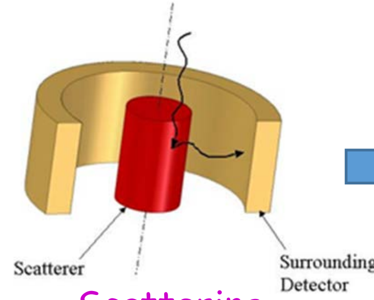

Scattering

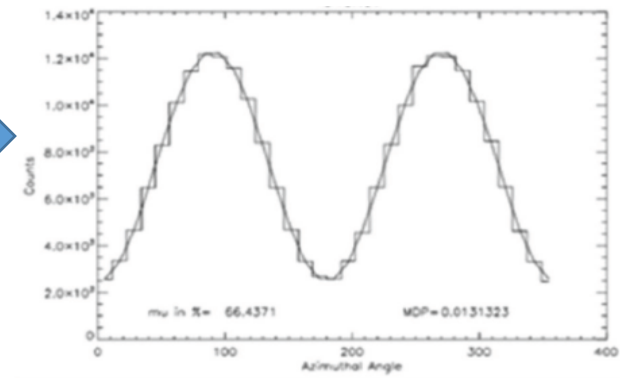

- Extremely difficult measurements
- Highly systematic prone → modulation amplitude is positive definite

The only well accepted polarization measurement of Crab nebula

Non optimized polarimetry → with multi element detector systems

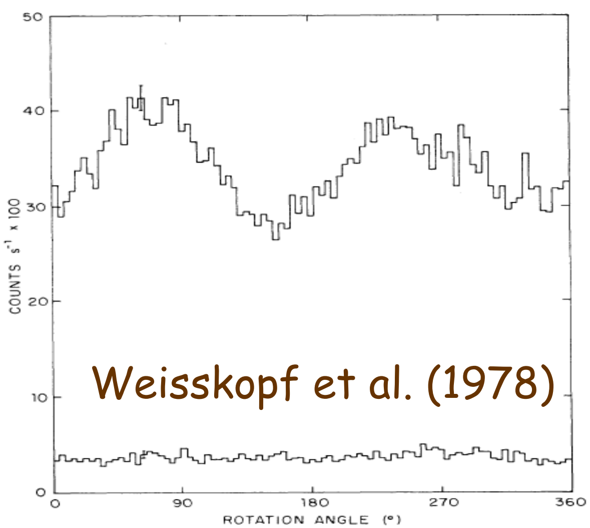

Weisskopf et al. (1978)

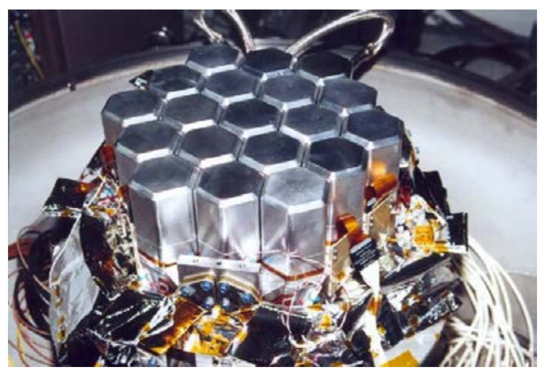

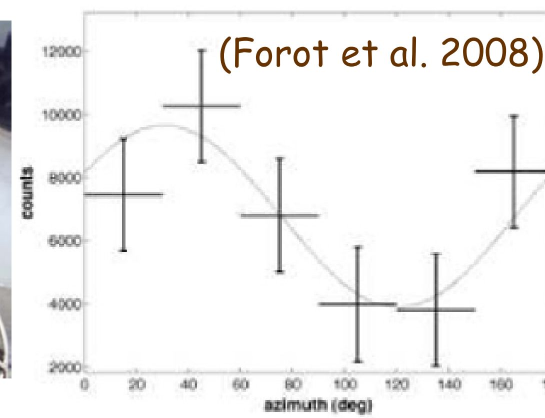

(Forot et al. 2008)

Many attempts, but controversial results
Main concern → not verified before launch

Hard X-ray Polarimetry with CZTI

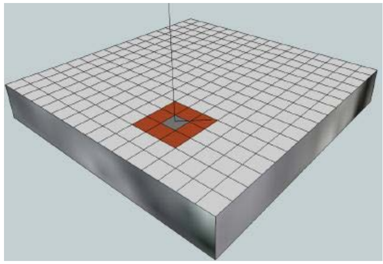

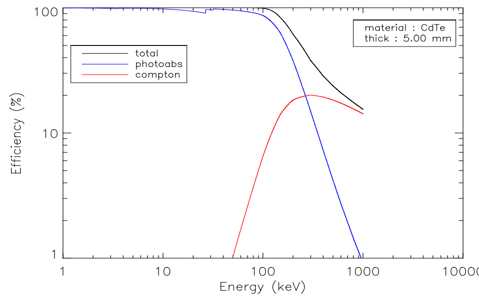

Not designed, but well tested for

Hard X-ray polarization easurements

- Compton polarimetry with double pixel events
- 100 – 380 keV energy range, due to ~30 keV pixel threshold
- Limited to very bright sources
- A significant addition to the nascent field of X-ray polarimetry

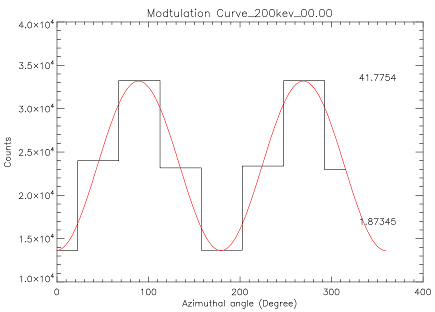

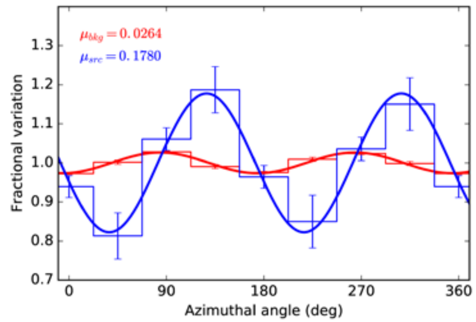

- Experimentally confirmed before launch
  - Also with unpolarized X-rays

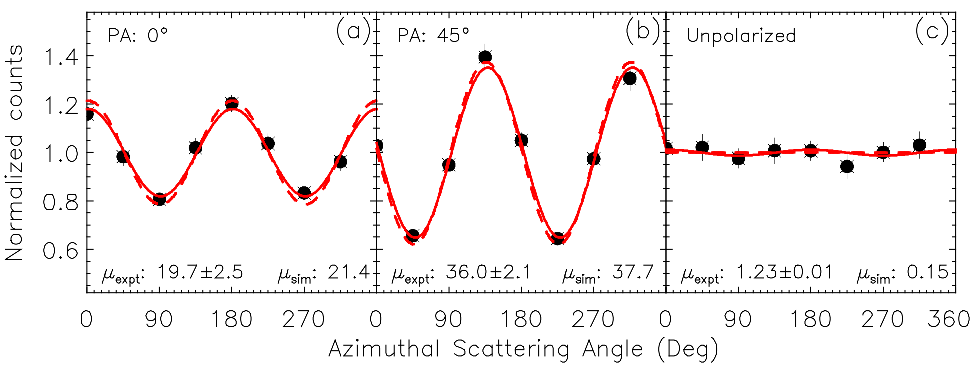

Vadawale et al. (2015)

Validation of event selection

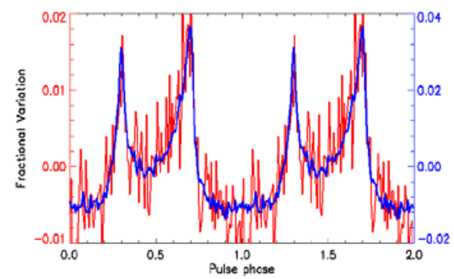

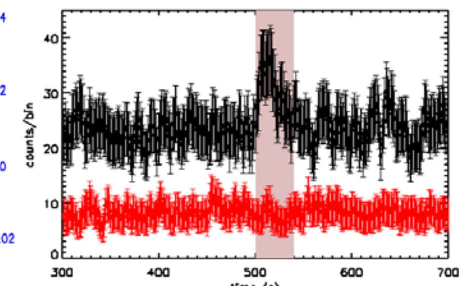

Background subtraction is the key

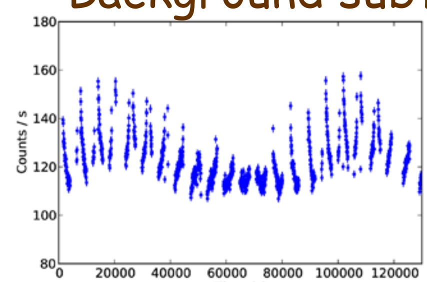

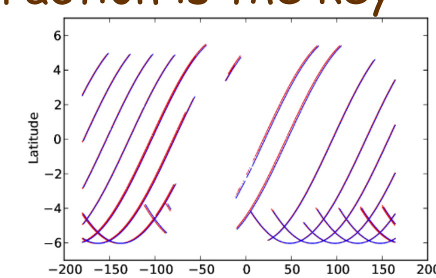

Crab Polarization Measurements with CZTI

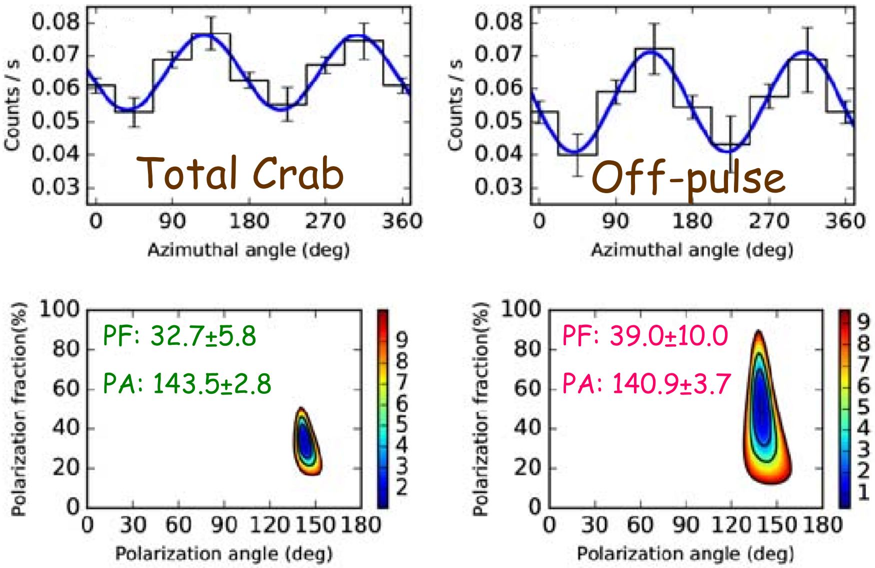

- Most sensitive (6σ) measurements in energy range 100 – 380 keV
- Broadly in agreement with available measurements at other energies
- Total 800 ks data used for 15 obs.

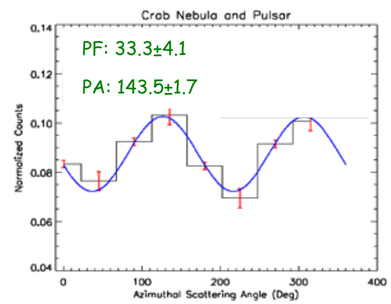

Improved significance (8σ) with ~1.8 Ms data

Phase Resolved Polarization Analysis

- Pulse period ➔ 33.7 ms
- Totally new results
- Significant variation in polarization during the off-pulse region

➔ New challenge for pulsar emission models

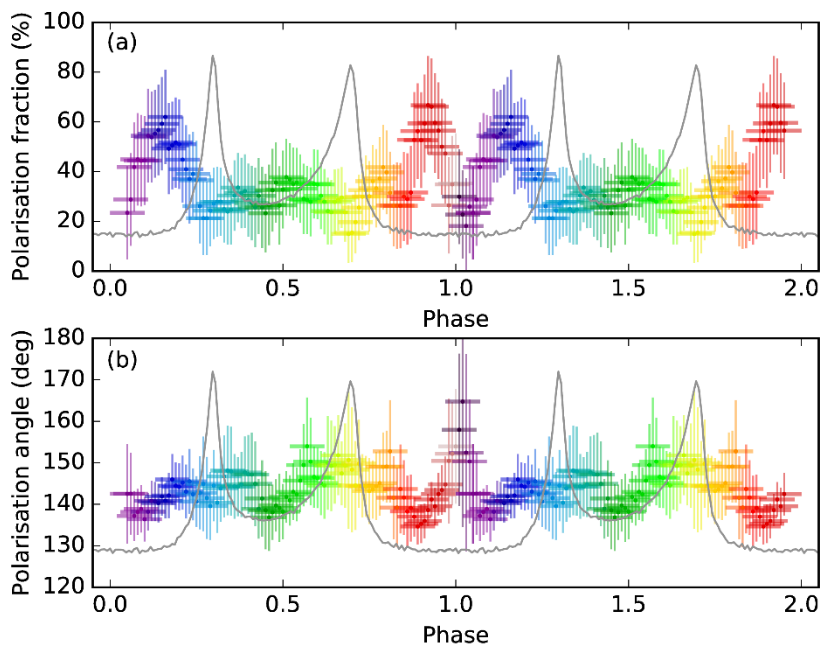

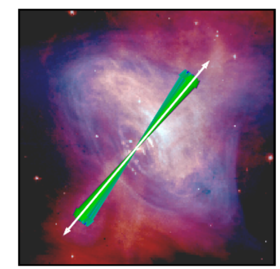

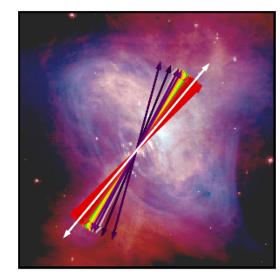

Vadawale et al. 2018 (Nature Astronomy)

Crab Hard X-ray Polarization

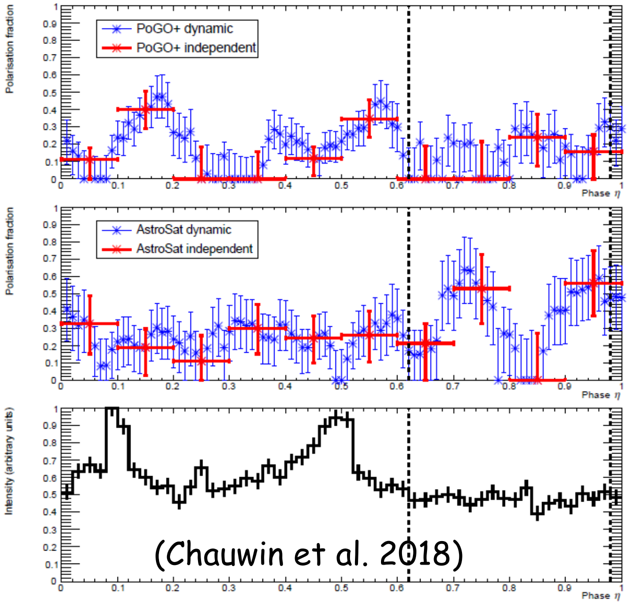

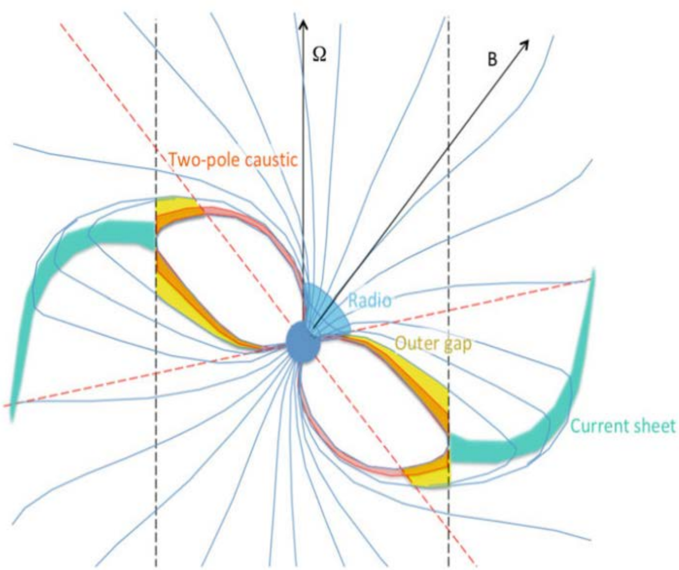

(Harding et al. 2019)

- New data confirms the strong variation of polarization in off-pulse region
- Re-analysis of POGO+ data → No significant variation in off-pulse variation
  - Due to strong energy dependence
- Only other phase resolved polarization measurement available in optical
  - Suggest Stripped-wind origin
- CZTI results broadly agrees with stripped wind origin
- Fundamental change in understanding of origin of X-ray emission

  → outside light cylinder!
- Need detailed modelling of phase dependent as well as energy dependent polarization properties at X-ray energies

CZTI as GRB Detector

CZTI as GRB Monitor

- Best effective area in energy range of 150 to 400 keV
- First GRB on first day / first observation
- More then 450 GRBs till now
- Rudimentary localization possible
  - Useful when no other option!

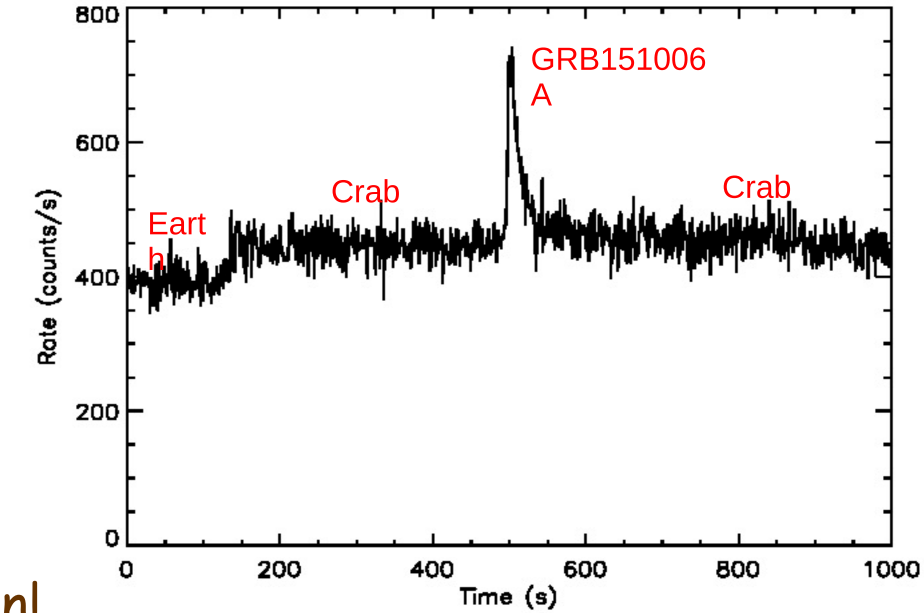

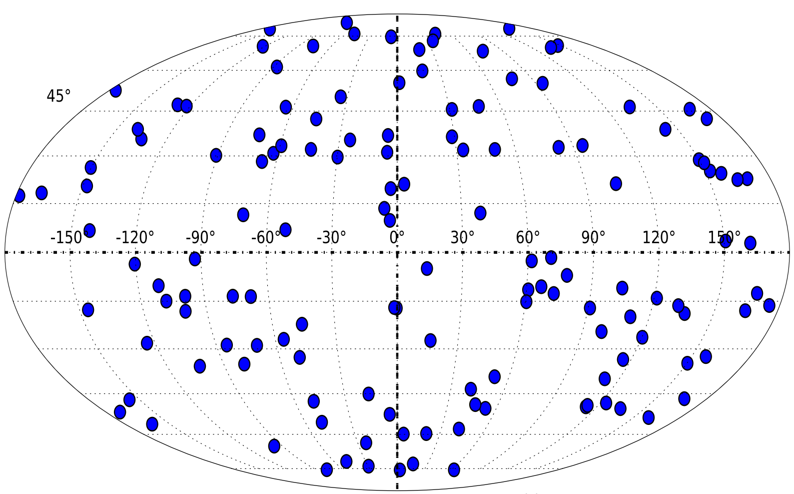

Till Feb. 2020

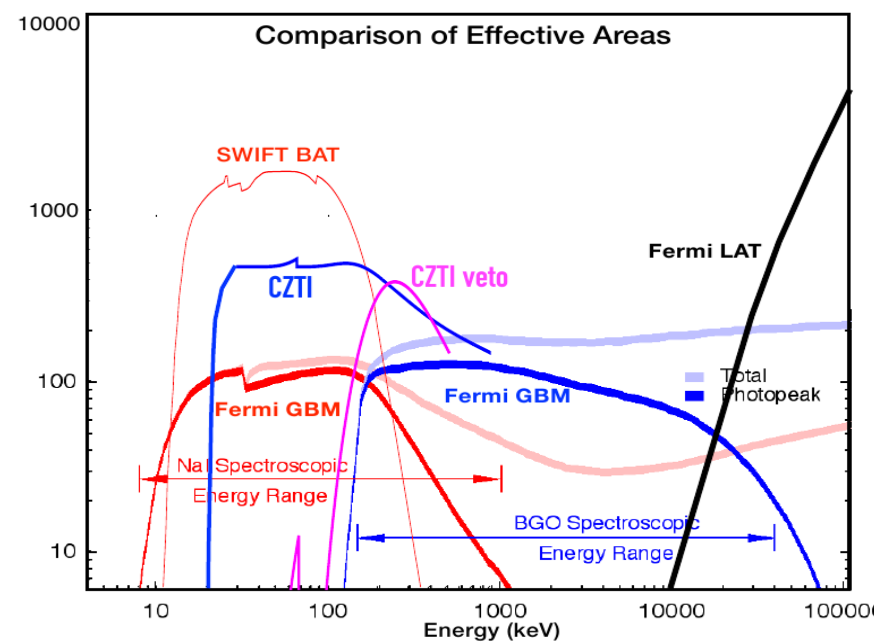

GRB Polarimetry

- Selection based on number of Compton events
  - 11 GRBs during first year (N_{COMPT} > 350)
  - Previous measurements available only for 10 GRBs → Doubling the sample one year
  - ~25 during next four years (more stringent selection)
- Modulation detection in GRB is relatively easy
  - Accurate background available pre / post GRB
  - High signal-to-noise

GRB Name	Compton events	PF (%)	PA (°)	Fluence(erg/cm^2)	T90 (Sec)	Peak energy (keV)
GRB 151006A	459	<79.2 ($\alpha = 0.05, \beta = 0.5$)	-	1.15E-5	203.9	227
GRB 160106A	950	68.5±24	-22.5±12.0°	4.526E-5	39.43	205
GRB 160131A	724	94±31	41.2±5.0°	3.26E-4	325	1152
GRB 160325A	835	58.75±23.5	10.9±17.0°	1.91E-5	64.9	235
GRB 160509A	460	96±40	-28.6±11.0°	2.90E-4	33.4	288
GRB 160607A	447	<75 ($\alpha = 0.05, \beta = 0.5$)	-	4.12E-5	379.65	176
GRB 160623A	1400	<46.4 ($\alpha = 0.05, \beta = 0.5$)	-	6.6E-4	90.46	562
		<57.1 ($\alpha = 0.01, \beta = 0.5$)				
GRB 160703A	448	<54.5 ($\alpha = 0.05, \beta = 0.5$)	-	2.7E-5	44.4	327
		<68.1 ($\alpha = 0.01, \beta = 0.5$)	-			
GRB 160802A	901	85±29	-36.1±4.6°	1.04E-4	16.4	284
GRB 160821A	2549	48.7±14.6	-34.0±5.0°	1.0E-5	43	968
GRB 160910A	832	93.7±30.92	43.5±4.0°	8.41E-5	24.3	347

(Chattopadhyay et al. 2019)

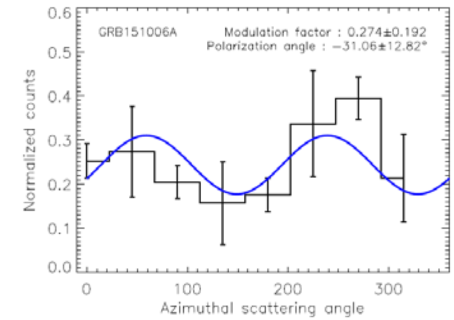

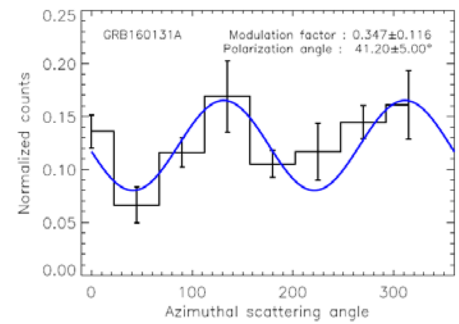

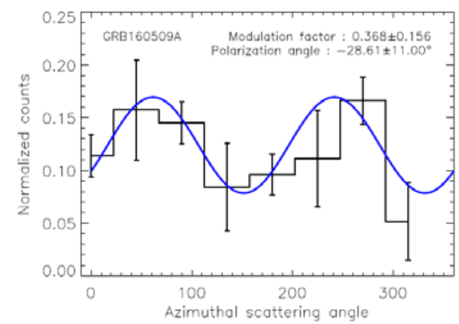

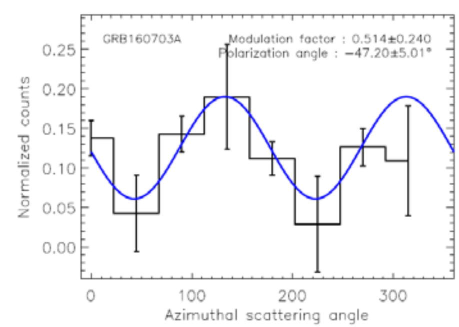

GRB Polarimetry

Off-axis polarimetry relies heavily on Geant4 simulations

- Validation of the AstroSat Mass Model

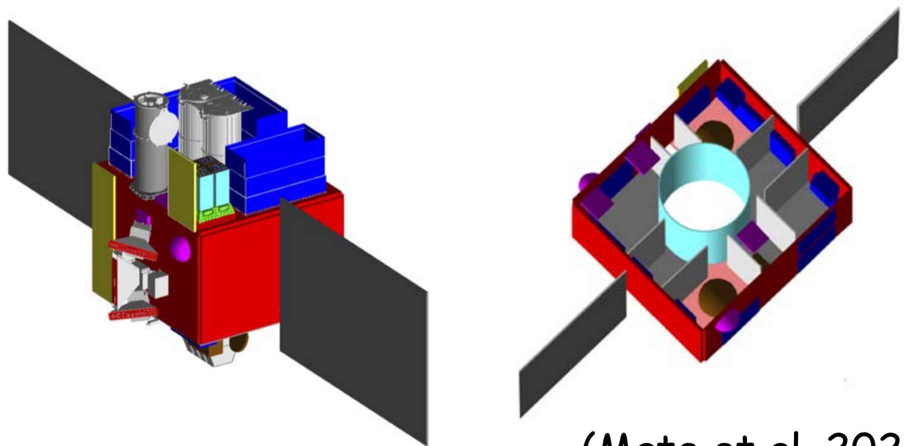

(Mate et al. 2021)

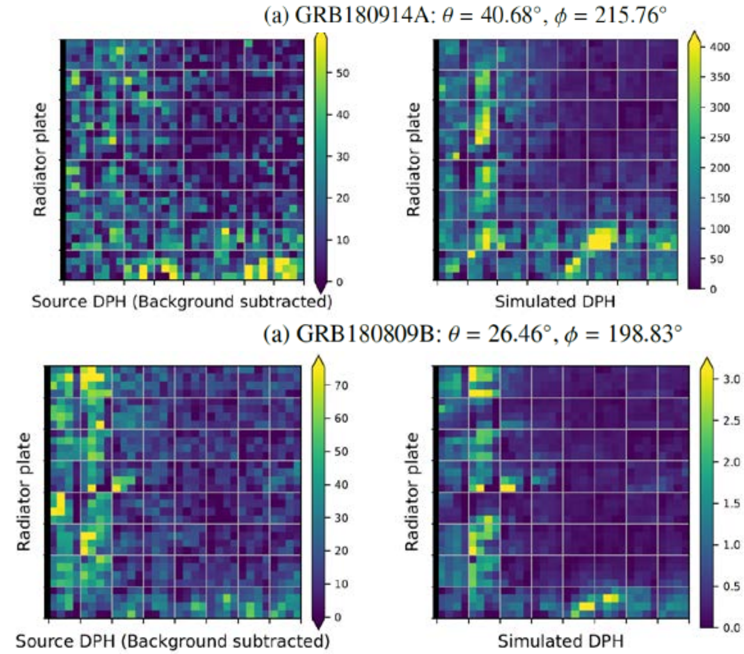

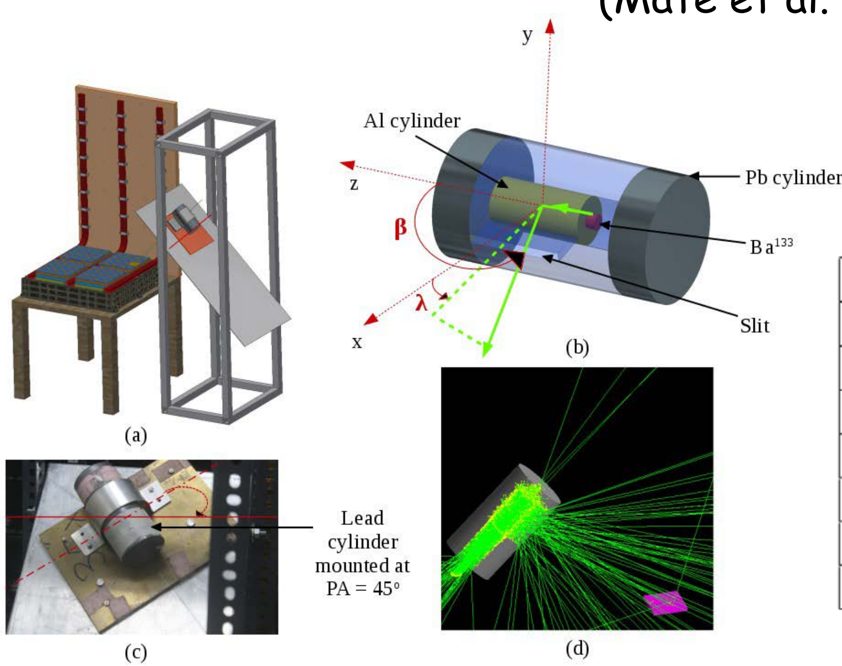

- Experimental confirmation of CZTI off-axis polarimetry

θ (°)	ϕ (°)	Incident PA (°)	PA_{expt} (°)	PF_{expt} (%)	PA_{sim} (°)	PF_{sim} (%)
30	0	0	0^{+3}_{-8}	52^{+7}_{-8}	0^{+6}_{-3}	40^{+7}_{-8}
30	0	20	15^{+5}_{-5}	75^{+10}_{-8}	10^{+5}_{-5}	78^{+10}_{-11}
45	0	0	0^{+1}_{-5}	63^{+5}_{-5}	0^{+5}_{-6}	65^{+6}_{-7}
45	0	20	20^{+3}_{-5}	80^{+6}_{-5}	10^{+2}_{-8}	79^{+10}_{-12}
45	45	45	45^{+5}_{-2}	74^{+4}_{-4}	40^{+10}_{-10}	60^{+6}_{-6}
60	0	0	0^{+4}_{-6}	74^{+4}_{-5}	5^{+2}_{-5}	74^{+4}_{-3}
60	0	20	15^{+4}_{-5}	93^{+3}_{-3}	15^{+5}_{-5}	84^{+5}_{-3}

(Aarthy et al. under review)

CZTI for EM-GW follow-up

Contributed to EM counterpart studies for at least two GW sources

- GW170104 → Prevented false alarm
- GW170817 → Enhanced confidence

ATLAS17aeu→

GRB170105A ✓

GW170104 ✗

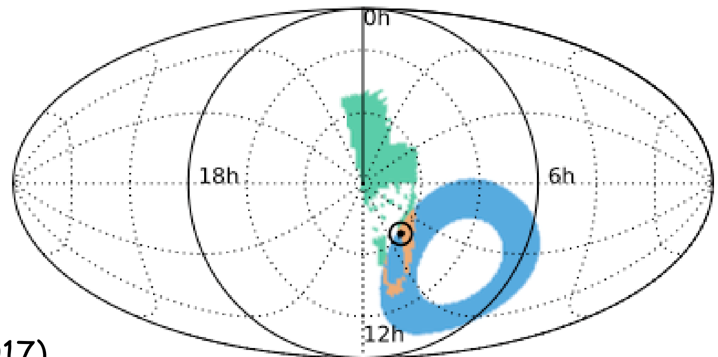

(Bhalerao et al., ApJ, 2017)

GW170817

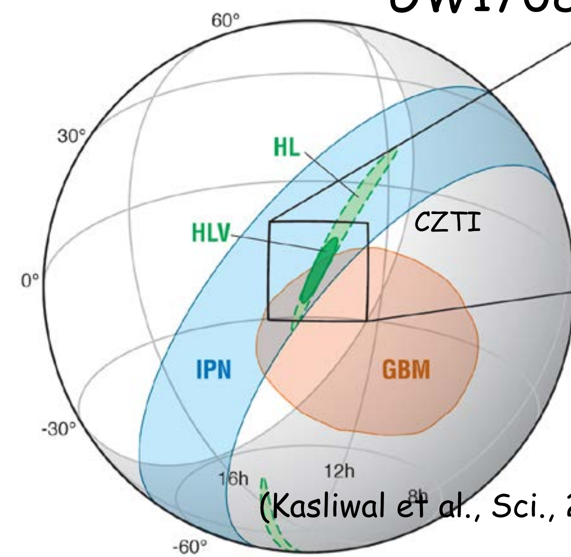

(Kasliwal et al., Sci., 2017)

GW170817 → BNS merger

- EM-counterpart was just on the sensitivity limit of present detectors
- Daily detection of such events in GW waves expected with network of 5 GW detectors
- Most of events likely to be missed by present / planned GRB detector
    - Sensitivity in EM band lagging behind GW!!

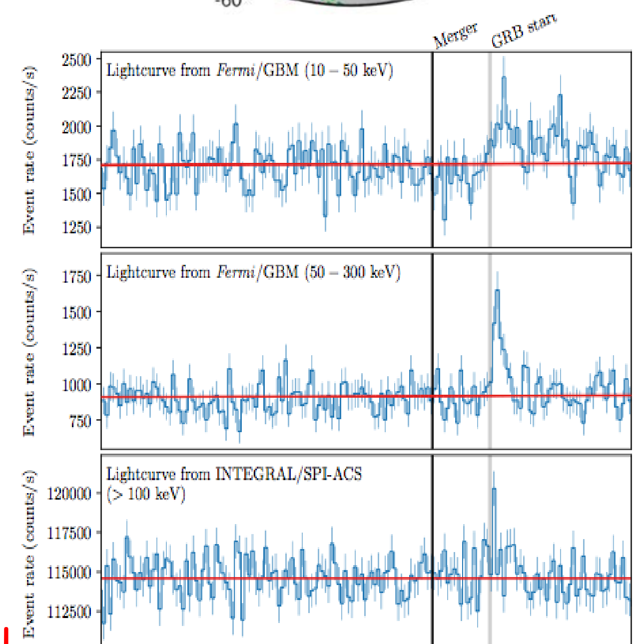

(LIGO Collaboration, ApJ, 2017)

DAKSHA – On Alert for High Energy Transients

- Small but ambitious mission on short time scale (~5 years)
- IIT-Bombay-PRL-TIFR-IUCAA joint program
  - ➔ Under consideration by ISRO

Scientific objectives:

- ***Detecting EM-counterparts of the Gravitational Wave sources***
- ***Wide band studies of GRB***

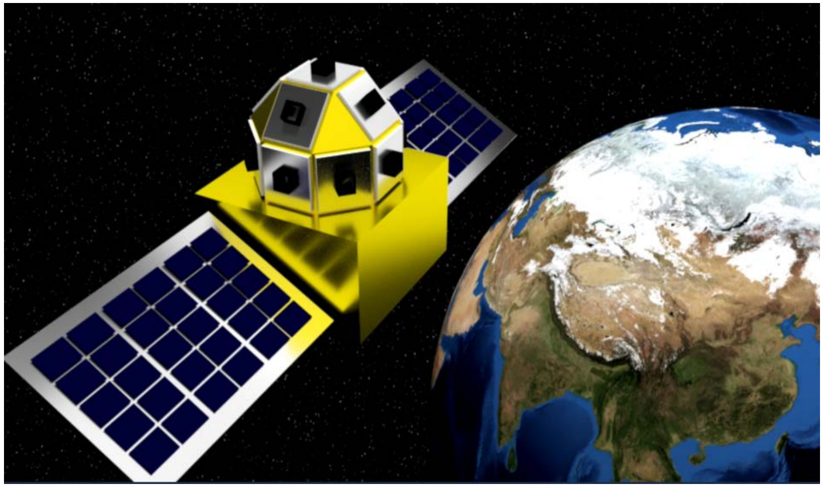

DAKSHA Key features:

- Order of magnitude more sensitive
- Continuous full Sky coverage (two S/C on LEO or one S/C in HEO)
- Sensitive GRB observations over wide spectral band (1 keV to 1 MeV) with three different types of detectors
  - SDD array with total effective area ~100 cm2 covering 1 – 40 keV
  - CZT detectors with effective area ~2000 cm2 covering 20 – 300 keV
  - Scintillator with eff. area of ~1600 cm2 covering 100 keV – 1 MeV

Summary

- CZTI is operating perfectly for more then five years now
  - Imaging / spectroscopy up to ~150 keV for bright sources
- CZTI is showing fantastic performance in its 'additional' capabilities
  - Proven to have good polarimetric capabilities in extended energy range of 100 – 300 keV
  - Accurate measurement of Crab hard X-ray polarization
  - First time phase resolved polarimetry of Crab
  - Interesting results on Cygnus X-1 in near future
- CZTI is also a prolific GRB detector
  - Very good GRB Polarimeter, large sample of GRBs

Thanks…